



Natural convection in metal foam heat sinks with open slots



Shangsheng Feng, Feichen Li, Fenghui Zhang, Tian Jian Lu*

MOE Key Laboratory for Multifunctional Materials and Structures (LMMS), Xi'an Jiaotong University, Xi'an 710049, PR China
State Key Laboratory of Mechanical Structure Strength and Vibration, Xi'an Jiaotong University, Xi'an 710049, PR China

ARTICLE INFO

Article history:

Received 16 March 2017

Received in revised form 29 June 2017

Accepted 14 July 2017

Available online 15 July 2017

Keywords:

Metal foam

Heat sink

Natural convection

Open slots

Optimum slot width

ABSTRACT

Natural convection in metal foam heat sinks with open slots was investigated experimentally. The test sample was made in-house by attaching several foam strips having fixed width of 10 mm and length of 100 mm onto a substrate of $100 \times 100 \times 4 \text{ mm}^3$ in size. A total of 29 test samples with different slot widths ($s = 0/2.86/5/8/12.5/20 \text{ mm}$) and foam heights ($H = 10/20/40/60/80 \text{ mm}$) were tested under both horizontal and vertical orientations for each sample. The zero width of open slots corresponds to a heat sink with a single foam block as considered in open literature, while the non-zero open slot width 2.86/5/8/12.5/20 mm corresponds to 8/7/6/5/4 foam strips in a heat sink, respectively. Compared to a single foam block, the foam with open slots are more permeable for air penetrating through the heat sink. More foam strips means more heat transfer area available but less permeation of the heat sink. Experimental results revealed that there exists an optimum open slot width (5–8 mm) for maximum heat transfer coefficient at given heat sink volume. With optimum open slot width, the heat transfer coefficient is enhanced by 14.9%, 21.3%, 37.6%, and 38.2% relative to single foam block ($s = 0 \text{ mm}$) at the foam height of 10 mm, 20 mm, 40 mm, and 80 mm, respectively.

© 2017 Published by Elsevier Inc.

1. Introduction

Thermal management is a key issue in electronic packaging as overheating can reduce the longevity and reliability of electronic components. Take LED (Light Emitting Diode) cooling for example, the operating temperature of LED chips usually should not exceed 100–110 °C [1], which is challenging given the high heat flux generated by the chips. Overheating can cause failure, reduction in lifetime, shifts in the emitted wavelength, and lower operational efficiency. Without appropriate thermal management, the efficiency of LEDs can be reduced from a theoretical value of 90% to values as low as 20% [2].

Although some advanced cooling schemes such as liquid cooling and two-phase cooling have been proposed, thermal management of electronics relies frequently on heat sinks with extended surfaces for heat transfer argumentation. The geometry of extended surfaces greatly determines the heat transfer area and flow properties within the structure. The ideal structure should have high fluid-solid interfacial area and high local heat transfer coefficient, but low flow resistance. However, the first two factors usually conflict with the last. Therefore, one must elaborately

design the structure of extended surfaces to balance the conflicting factors to achieve maximum heat transfer under specific conditions.

State-of-the-art heat sinks for natural convection often use application-specific fin structures as extended surfaces, such as parallel straight fins [3,4], radial straight fins [5,6], tree-shaped straight fins [7], pin-fins [8], pin-fins with venting holes [9], etc. Besides the above mentioned fin structures, porous media have also been used as extended surfaces for decades as motivated by their large surface area densities. Natural convection in packed beds and granular porous media with porosities in the range of 0.3–0.5 can be referred to Refs. [10,11]. Open-cell metal foams, however, possess a much higher porosity ($\varepsilon > 0.9$) enabling a higher permeability and more lightweight heat sinks than those constructed with packed beds. Due to these significant advantages, metal foams have become increasingly attractive for the cooling of LEDs in automotive and domestic applications [12].

Natural convection in metal foams has been extensively studied in the past few years. Various factors including pore density, porosity, foam height, orientation, and local thermal non-equilibrium have been explored. Bhattacharya and Mahajan [13] experimentally investigated natural convection in metal foams and finned metal foams having different pore densities (5, 10, 20, 40 pores per inch, PPI) and porosities (0.89–0.96). The size of the tested samples was fixed at $6.25 \text{ cm} \times 6.25 \text{ cm} \times 5 \text{ cm}$

* Corresponding author at: MOE Key Laboratory for Multifunctional Materials and Structures (LMMS), Xi'an Jiaotong University, Xi'an 710049, PR China.

E-mail address: tjlu@mail.xjtu.edu.cn (T.J. Lu).

Nomenclature

b	width of each foam strip (mm)	T_{am}	ambient temperature (K)
h	heat transfer coefficient ($\text{W}/\text{m}^2 \text{K}$)	T_f	air temperature (K)
H	height of foam strip or heat sink (mm)	ΔT	temperature difference (K)
L	length of foam strip or heat sink (mm)		
N	number of foam strips		
Q_{in}	heat input (W)	<i>Greek symbols</i>	
Q_{loss}	heat loss (W)	ε	porosity
T_w	substrate temperature (K)		

(length \times width \times height). The results showed that, for a given porosity, the heat transfer rate is enhanced for larger pore sizes (less pore densities) due to higher permeability and hence higher entrainment of air through the porous medium. For a given pore density, the heat transfer performance increases with decreasing porosity due to the increase in effective thermal conductivity.

Hetsroni et al. [14] experimentally measured natural convection in metal foam strips with internal heat generation using IR technique. It was found that natural convection is more enhanced by a 20 PPI metal foam, although its specific surface area is lower than that of the 40 PPI metal foam, which is consistent with the finding of Bhattacharya and Mahajan [13]. Also, thermal non-equilibrium between the solid skeleton and air was found to be significant through image processing of thermal maps on both the surface and the inner region of the metal foam specimen.

Schamphelire et al. [15] experimentally studied natural convection in slender metal foams with length 254 mm and width 25.4 mm. With a fixed porosity of 0.93, the height of 10 PPI foam was varied as 6/12/18/25.4/40 mm, while that for 20 PPI foam as 6/12/18 mm. It was found that the 10 PPI foam performed up to 25% better in heat transfer compared with the same-dimensioned 20 PPI foam. Increasing the foam height resulted in an increase in heat transfer rate, but this increment was reduced for larger foam heights. This was attributed to increased flow resistance due to the buoyancy-driven air flow in upward direction and reduced foam efficiency.

Qu et al. [16] experimentally investigated natural convection in copper foams with different pore densities (10–40 PPI), porosities (0.90–0.95), and heights (10–50 mm). Experiments were run for each sample at inclination angles of 0 (vertical orientation), 15, 30, 45, 60, 75, 90 (horizontal orientation). Again, the results showed that the heat transfer rate increased with decreasing pore density and porosity, regardless of the orientation and height. The heat transfer was enhanced by increasing foam height due to increased surface area.

Zhao et al. [17] presented a combined experimental and numerical study of Rayleigh-Benard natural convection in enclosed metal foams that were heated from the below. The experimental results showed that natural convection is very significant, accounting for up to 50% of the effective foam conductivity obtained at ambient pressure. The numerical results further revealed that the effective foam conductivity increases with the Darcy number, indicating that natural convection in metal foams was promoted by higher permeability.

Phanikumar and Mahajan [18] numerically and experimentally investigated natural convection in metal foams of 6.35 cm \times 6.35 cm \times 5.08 cm (length \times width \times height) positioned in a large Plexiglas housing. The experimental results for aluminum foams in air showed that heat transfer rate decreases as the pore density is increased from 5 to 40 PPI, and for a given PPI, the heat transfer increases with decreasing porosity. The numerical results revealed that the flow enters into the foam from the side surfaces, penetrating through the foam along the upward

direction due to buoyancy force. Increasing the Darcy number (permeability) helps the flow to penetrate deeper into the porous layer. At a lower Darcy number, although the Rayleigh number is relatively high, the flow is unable to penetrate deeper as the resistance is higher.

Literature studies [13–18] consistently concluded that heat transfer rate in a low pore density foam is more enhanced, although its surface area is less than that of a high pore density foam having the same porosity and geometrical dimensions. This demonstrates that fluid permeation plays a dominant role in the heat transfer rate. As a consequence, in order to enhance the heat transfer, increasing the overall permeation of a metal foam heat sink becomes the key issue. To this end, this paper proposed a novel metal foam heat sink with open slots and investigated its natural convection characteristics experimentally. In comparison, literature studies have mainly considered natural convection in a single metal foam block, i.e., without open slots. It is expected that by introducing open slots in the metal foam, the penetration of fresh air into the heat sink would be promoted, thus enhancing the overall heat transfer rate. The present experimental study then systematically addresses the following questions: How many open slots should be introduced? At a given volume of heat sink, does there exist an optimum slot width for maximum heat transfer? Will this optimum width vary with the height and orientation of heat sink? How will the height and orientation affect natural convection in this type of heat sink?

2. Experimental details

2.1. Test samples and heating assembly

All the test samples were fabricated in-house with copper foam with fixed pore density of 5 PPI (pores per inch) and fixed porosity of 0.91. The copper foam block was first cut into strips of fixed width and length ($b \times L = 10 \times 100$ mm) but varying height ($H = 10/20/40/60/80$ mm) using a precision wire cutting machine. Then the foam strips were bonded onto an aluminum substrate ($100 \times 100 \times 4$ mm³) using a high conductivity thermal adhesive (Arctic Silver™, $k > 8.8$ W/mK) to minimize the contact thermal resistance. The contact thermal resistance with a high conductivity thermal adhesive was found to be negligible compared to the overall thermal resistance of heat sink if the foam strips were perfectly contacted with the substrate [19,20].

The number N of the foam strips was varied as 4/5/6/7/8/10. Correspondingly, the width of the open slots (or spacing s between adjacent foam strips) varied as 20/12.5/8/5/2.86/0 mm. For a heat sink with 10 foam strips, no gap existed between adjacent foam strips. In this case, the heat sink reduced to the one considered extensively in open literature, heat sink with a single foam block. The height of foam strips (or heat sink height, H) was varied as 10/20/40/60/80 mm. In total, 29 heat sinks with different open slot widths and heights were fabricated and tested.

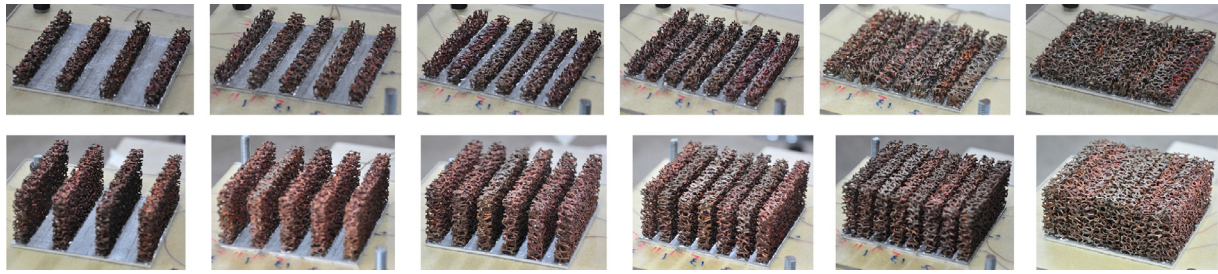


Fig. 1. Selected test samples of height $H = 10$ mm (top) and $H = 40$ mm (bottom), with 4/5/6/7/8/10 foam strips for each height.

Fig. 1 shows the photos of selected heat sinks with 10 mm (top) and 40 mm (bottom) in height, with 4/5/6/7/8/10 foam strips for each height. Table 1 lists the parameters of all the heat sinks tested in the current study.

Fig. 2 shows schematically the heating and thermal insulation assembly. Three slots were cut from the lower surface of the substrate with a cross-sectional area of 1×1 mm². Five 36-gauge T-type bead thermocouples (Omega, wire diameter: 0.127 mm) were embedded in the slots to measure the average temperature of the substrate. The remaining gaps of the three slots were then filled with thermal grease to ensure the lower surface of the substrate was flat. A film heating pad was subsequently attached to the lower surface of the substrate to apply uniform heat flux boundary condition. The heat sink with heating pad was then placed onto a 75 mm thick thermal insulation foam (polyurethane, $k \sim 0.036$ W/mK). A Perspex frame having the same thickness as that of the substrate (4 mm) was connected to the insulation foam using four screws at the corners. Finally, the heat sink was fixed to the Perspex frame by applying glue at the four edge surfaces of the substrate.

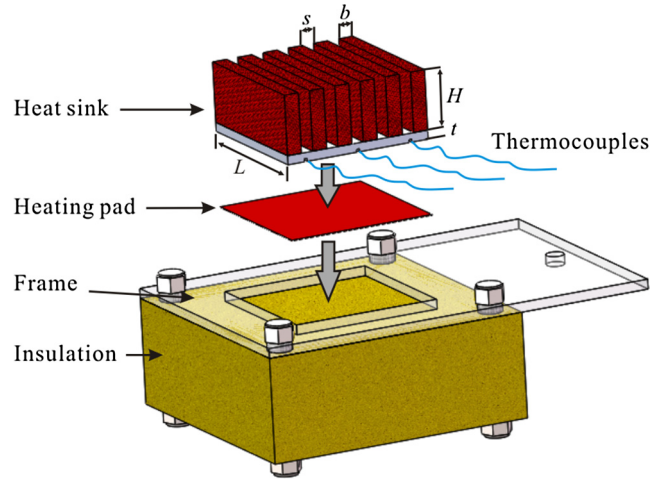


Fig. 2. Schematic of heating and thermal insulation assembly.

2.2. Experimental setup

Fig. 3 displays schematically the experimental apparatus. To avoid fluctuation of the ambient temperature, the test samples were placed in an enclosed space of $1.5 \text{ m} \times 1.5 \text{ m} \times 2 \text{ m}$. The ambient temperature in the enclosed space was measured using two T-type bead thermocouples located far away from the test samples to avoid the influence of the hot plume from the heat sinks on the ambient temperature measurement. A DC power supply (Agilent) was used to provide electricity for the film heating pad. The heat input was varied from 0.8 to 24 W in experimental runs. A data acquisition system (Agilent, 34970A) was employed to record signals from the five thermal couples (measuring the

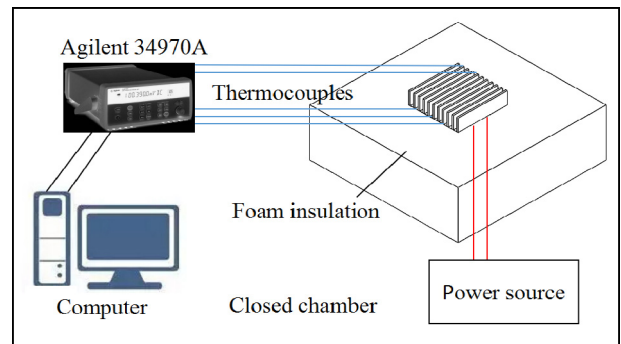


Fig. 3. Schematic of experimental setup.

Table 1
Parameters of heat sink samples.

No.	Height (mm)	Slot width (mm)	Number of foam strips (-)	No.	Height (mm)	Slot width (mm)	Number of foam strips (-)
1	10	0	10	16	40	8	6
2	10	2.86	8	17	40	12.5	5
3	10	5	7	18	40	20	4
4	10	8	6				
5	10	12.5	5	19	60	2.86	8
6	10	20	4	20	60	5	7
7	20	0	10	21	60	8	6
8	20	2.86	8	22	60	12.5	5
9	20	5	7	23	60	20	4
10	20	8	6	24	80	0	10
11	20	12.5	5	25	80	2.86	8
12	20	20	4	26	80	5	7
13	40	0	10	27	80	8	6
14	40	2.86	8	28	80	12.5	5
15	40	5	7	29	80	20	4

substrate temperature) and another two thermocouples (measuring the ambient temperature in the enclosed space). All the thermocouples have been calibrated in advance by testing the temperature of ice-water mixture: the tested temperatures were within ± 0.15 °C, proving the accuracy of the temperature measurements. The heating and thermal insulation assembly was placed on a platform that allows the heat sink to be positioned in horizontal or vertical orientation, as shown in Fig. 4(a) and (b), respectively.

In order to explore the thermal-fluid flow behavior in metal foam heat sinks with open slots, the distribution of air temperature on top of the heat sink was measured. For such purpose, a 36-gauge T-type thermocouple was housed into a stainless steel tube having an inner diameter of 1 mm and an outer diameter of 1.2 mm. Then the tube was bent into L shape, forming a temperature probe. The temperature probe was mounted on a 1-dimensional linear traverse system to measure the temperature distribution along the mid-span of heat sink in lengthwise direction, as shown in Fig. 4(a). The thermocouple bead of the probe was located 5 mm above the tip of the heat sink.

2.3. Experimental heat transfer coefficient

The heat transfer coefficient was defined as,

$$h = \frac{Q}{A\Delta T} = \frac{Q_{in} - Q_{loss}}{A(T_w - T_{am})} \quad (1)$$

where A was the heated area of the substrate, and T_w and T_{am} were average substrate temperature and ambient temperature,

respectively. Q_{in} ($=UI$) was the power input and U and I were voltage and current readings from the DC power supply, respectively. Q_{loss} was the heat loss estimated in Section 2.4.1.

Heat transfer coefficients of the 29 test samples listed in Table 1 were measured with varying the heat inputs. Since each test sample was run in both horizontal and vertical orientations, 58 test cases were carried out in this study. As each test case included 5 data points for different heat inputs, there were in total 290 data points. Each data point took around 3 h to achieve steady state. Steady state was judged if the temperature change of each thermocouple reading was less than 0.2 K in ten minutes.

Selected test cases were repeated to verify the reproducibility of the test setup. Fig. 5 shows the comparison of data separately measured at two different times for the test cases of (a) $H = 80$ mm, 4 fins, horizontal orientation; and (b) $H = 80$ mm, 7 fins, horizontal orientation. The maximum deviation of experimental data in Fig. 5 (a) is 4%, which is slightly higher than the estimated uncertainty of the heat transfer coefficient (2.3%). This may be explained by the different thermal radiation contributions due to different ambient temperatures. The deviation of experimental data in Fig. 5(b) is well within the estimated uncertainty of the heat transfer coefficient.

2.4. Heat loss and uncertainty analysis

2.4.1. Heat loss analysis

The thermal input of the heating pad was dissipated mainly by the heat sink and partially by heat loss through

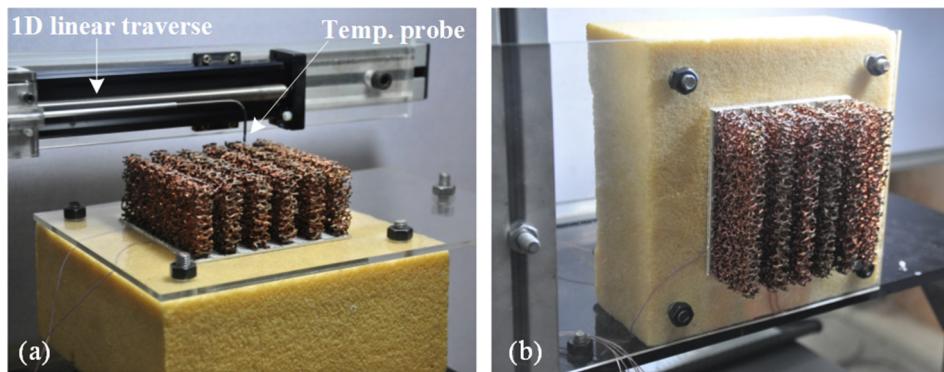


Fig. 4. Heat sink positioned in horizontal (a) and vertical (b) orientations.

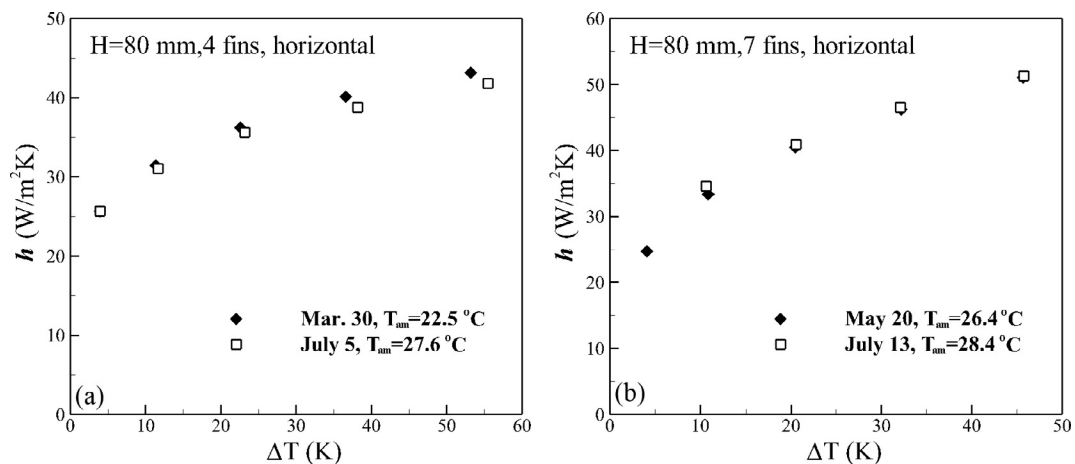


Fig. 5. Comparison of experimental data separately measured at different times for (a) $H = 80$ mm, 4 fins, horizontal orientation; and (b) $H = 80$ mm, 7 fins, horizontal orientation.

the insulation foam and Perspex frame. To estimate the heat loss, natural convection from a flat plate of the same material make and same dimensions as the heat sink substrate was tested. The heating and thermal insulation assembly as well as the experimental setup were identical to those described in Sections 2.1 and 2.2. For the flat plate, the thermal input of the heating pad was dissipated via: (1) heat dissipation from flat plate surface to ambient by natural convection and radiation (Q_p), and (2) heat loss, as depicted in Fig. 6. Because Q_p can be calculated using well established correlations for natural convection and radiation from a flat plate [21], the heat loss was then calculated and correlated as a function

of temperature difference between the substrate and the ambient, as:

$$Q_{loss} = Q_{in} - Q_p = -9E - 05 \times \Delta T^2 + 0.0202 \times \Delta T \quad (2)$$

Eq. (2) was then used to estimate the heat loss from the heat sinks with metal foam. For all the heat sinks tested in the study, the heat loss accounted for 3–15% of the total heat input.

2.4.2. Uncertainty analysis

The main uncertainties in this experiment were due to errors in measurements of power, thermocouple readings, physical dimensions, and heat loss. According to the method of Kline and McClintock [22], the uncertainty of the heat transfer coefficient defined in Eq. (1) can be calculated, as:

$$\frac{\delta h}{h} = \sqrt{\left(\frac{\delta Q_{in}}{Q_{in} - Q_{loss}}\right)^2 + \left(\frac{\delta Q_{loss}}{Q_{in} - Q_{loss}}\right)^2 + \left(\frac{\delta A}{A}\right)^2 + \left(\frac{\delta T_w}{T_w - T_{am}}\right)^2 + \left(\frac{\delta T_{am}}{T_w - T_{am}}\right)^2} \quad (3)$$

The error associated with the voltage and current measurement was 0.5% as provided by the manufacturer. This resulted in an error of 1.5% in the estimation of the heat input Q_{in} . The error of heat loss was estimated according to eq. (2) as 0.1% which was negligible. The error in measurement of the cross-sectional area was estimated to be 1%. The error for the thermocouple readings was estimated to be 0.3 °C. For typical temperature differences observed in our experiments of the order of 30 K, the error in temperature measurement was 1%. With each error source determined, the total error was estimated to be 2.3% according to Eq. (3).

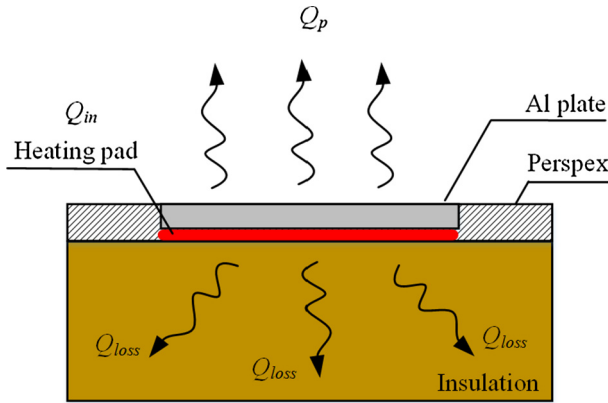


Fig. 6. Heat loss estimation.

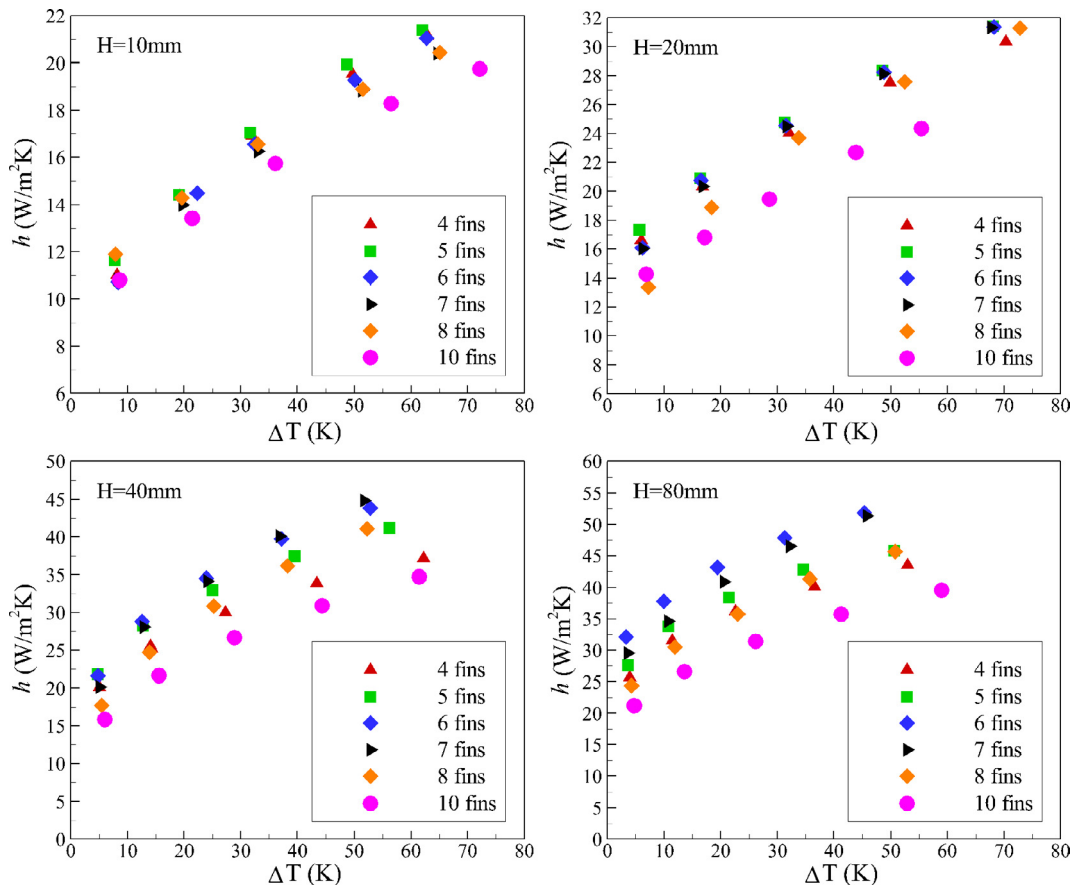


Fig. 7. Heat transfer coefficient plotted as a function of temperature difference for selected number of foam strips (or width of open slots) at foam height of 10/20/40/80 mm; horizontal orientation.

3. Results and discussion

3.1. Effect of open slot width

With the width of foam strip (b) fixed at 10 mm, the number of the foam strips was gradually increased from 4 to 10 to quantify the effect of slot width between adjacent foam strips on natural convective heat transfer. The heat sinks with four foam strips had the largest slot width ($s = 20$ mm), while those with ten foam strips had zero width ($s = 0$ mm) corresponding to a single foam block. Fig. 7 plots the heat transfer coefficient as a function of temperature difference, with the height of foam strips varying as 10, 20, 40, 80 mm, respectively. For all the heights investigated, an optimum number of foam strips for maximum heat transfer was found to exist, and heat sinks with ten foam strips (single foam block) exhibit the worst performance. The optimum number of foam strips was found to be 5, 5/6/7, 6/7, and 6 for foam height of 10 mm, 20 mm, 40 mm, and 80 mm, respectively. As shown in Fig. 7, at $H = 20$ mm, heat sinks with 5/6/7 foam strips have similar and the best performance; while at $H = 40$ mm, heat sinks with 6/7 foam strips have similar and the best performance. With a fixed temperature difference of 50 K, the heat transfer coefficient of heat sinks with the optimum number of foam strips is 14.9%, 21.3%, 37.6%, and 38.2% larger than the counterpart heat sinks with a single foam block at height of 10 mm, 20 mm, 40 mm, and 80 mm, respectively.

In order to better show the effects of slot width, the heat transfer coefficient was plotted as a function of slot width for selected foam heights (10/20/40/60/80 mm) at a fixed temperature difference of 50 K. The heat transfer coefficients of different heat sinks at the fixed temperature difference were obtained from linear interpolation. As shown in Fig. 8(a) for horizontal orientation and Fig. 8(b) for vertical orientation, the heat transfer coefficient first increases then decreases as the slot width is increased, and there exists an optimum width of 5–8 mm. However, at lower foam heights (e.g., $H = 10/20$ mm), the heat transfer coefficient is less sensitive to changes in slot width. The above findings hold for both the horizontal and vertical orientation cases.

As the number of foam strips increases, the total heat transfer area is increased, while the fresh air is more difficult to penetrate into the foam due to reduced spacing between adjacent foam strips. Consider then two extreme cases: (1) without any foam strip, the extended surface area is zero; (2) with ten foam strips, the fresh air is difficult to reach the center bottom of the foam especially when the heat sink is tall. The contradiction between extended surface area and accessibility to fresh air leads to the

existence of optimum foam strip number. For relatively short heat sinks of metal foam with open slots (e.g., $H = 10/20$ mm), heat transfer from the unfinned substrate becomes more important compared to that from the extended surface of foam. This explains why the overall heat transfer coefficient of short heat sinks is less sensitive to changes in slot width, as shown in Fig. 8.

3.2. Effect of foam height

Fig. 9(a) plots the heat transfer coefficient as a function of foam height for the horizontal orientation, with the temperature difference fixed at 50 K. Fig. 9(b) presents the corresponding results for the vertical orientation. For both orientations, the heat transfer coefficient increases with increasing foam height while all other parameters remain unchanged. This is attributed to the larger heat transfer area available for heat sinks with higher foam height.

However, the rate of enhancement decreases as the height is increased. For the horizontal case, there are two potential factors contributing to the decline in heat transfer enhancement. First, the fin efficiency decreases with increasing foam height due to the low effective thermal conductivity of high porosity foam, estimated to be 12 W/mK for the tested copper foam [23]. Second, the flow resistance also increases because the flow travels through the foam in the upward direction. For the vertical case, only the first factor holds as the second factor can be neglected. Since decreasing trend in heat transfer enhancement with increasing height was observed for both horizontal and vertical orientations, therefore the major factor contributing to this phenomenon may be the low effective conductivity of metal foam.

3.3. Heat transfer comparison between horizontal and vertical orientations

Fig. 10 compares the heat transfer coefficients between horizontal and vertical orientations for heat sinks with ten foam strips; the foam height is varied as 10 mm, 20 mm, 40 mm, and 80 mm. Similar comparison results are shown in Fig. 11 for heat sinks with six foam strips but varying height of 10 mm, 20 mm, 40 mm, and 80 mm. As shown in Figs. 10 and 11, overall, the heat transfer coefficient of horizontal orientation is higher than that of vertical orientation for the same heat sink. Regardless the orientation of the heat sink positioned, the heated air flow in the foam always rises along the adverse direction of gravity. The heated air flow in vertically positioned heat sinks should travel along the length of the heat sink ($l = 100$ mm), which may be longer than that in the same heat sink positioned horizontally ($l < 80$ mm, i.e., the maximum

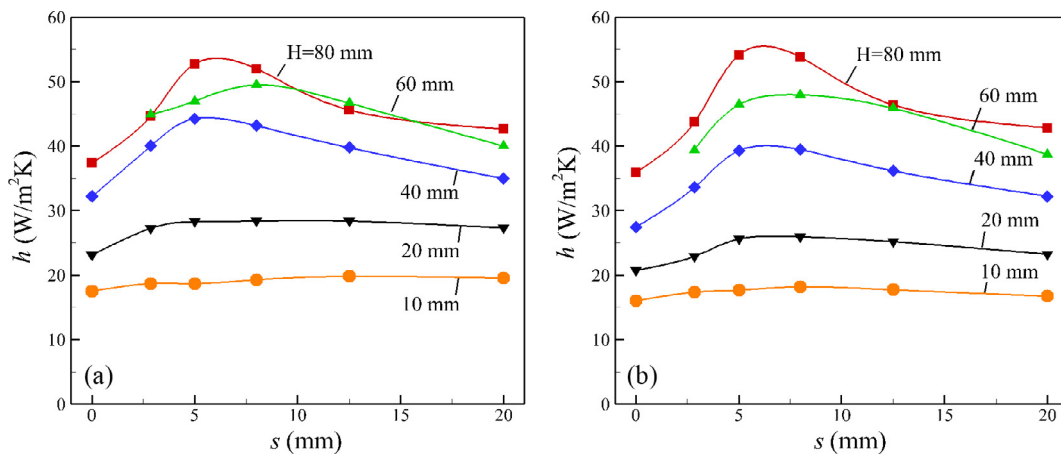


Fig. 8. Heat transfer coefficient plotted as a function of open slot width for selected foam heights at horizontal orientation (a) and vertical orientation (b); $\Delta T = 50$ K.

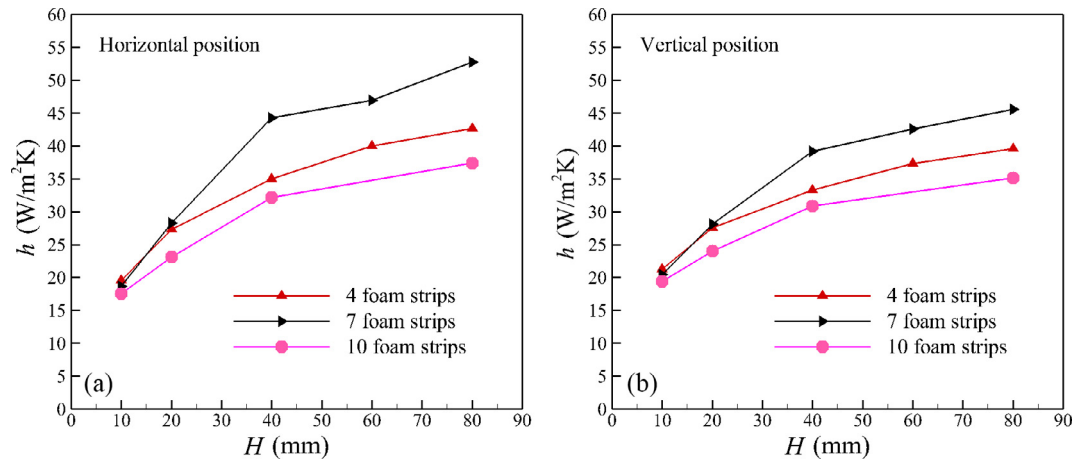


Fig. 9. Heat transfer coefficient plotted as a function of foam height for selected foam strip numbers: (a) horizontal orientation and (b) vertical orientation; $\Delta T = 50$ K.

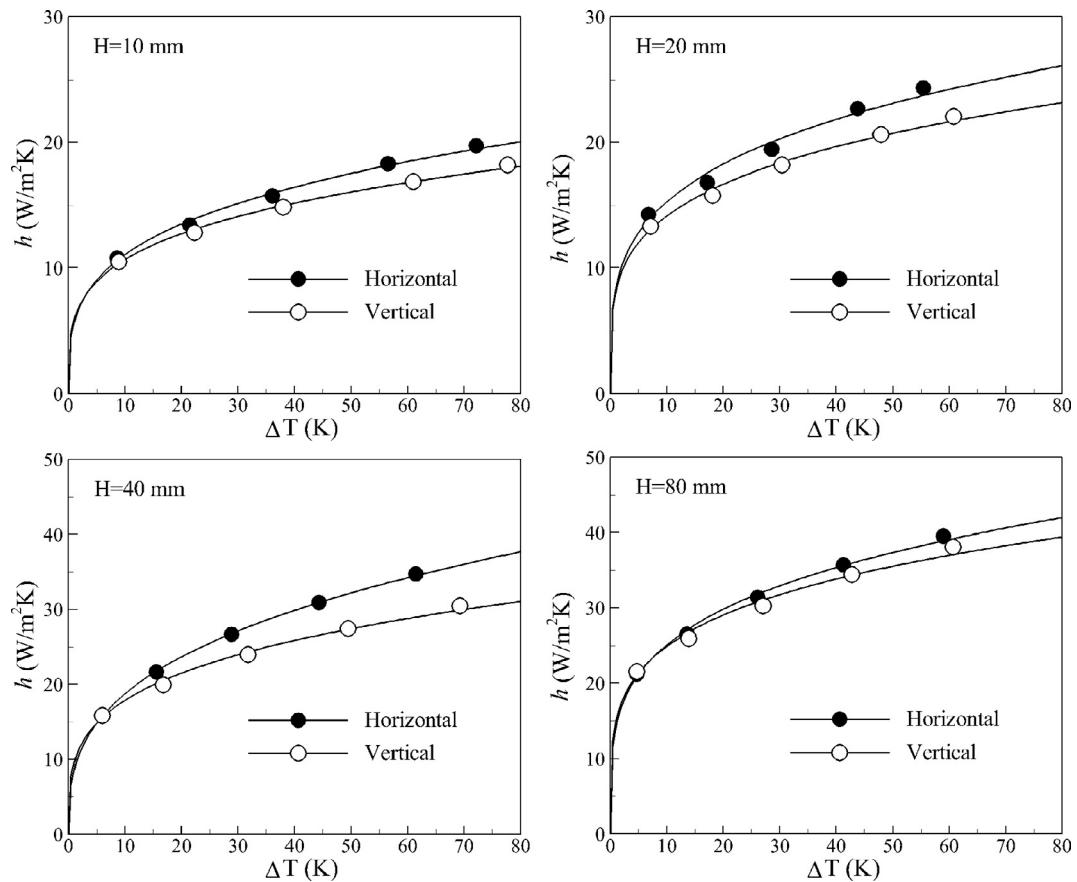


Fig. 10. Comparison of heat transfer coefficients between vertical and horizontal orientations for selected foam heights of 10/20/40/80 mm, with foam strip number $N = 10$.

height investigated). This may cause larger flow resistance in the vertical heat sink, thus degrade its heat transfer performance as shown in Figs. 10 and 11.

3.4. Thermal-fluid flow characteristics

To reveal the thermal-fluid flow characteristics in heat sinks finned by metal foam with open slots, the distribution of air temperature above the foam tip was measured using a temperature probe for a horizontally positioned heat sink with 6 foam strips and a height of 40 mm. Fig. 12 displays the dimensionless temper-

ature distribution across two foam strips. It is seen that the air temperature peaks at the center top of a given foam strip while dips at the center of a given open slot (channel), suggesting that the hot plume (or rising air flow) is right on top of the foam rather than on top of the channel. According to this temperature distribution, the flow picture in the heat sink may be sketched as shown in Fig. 12. The fresh air enters the heat sink horizontally from the ends of open slots (channels) and then penetrates into foam strips from the open channel. Subsequently, the flow is heated and rises in the foam strips due to interstitial heat transfer and buoyancy force. Eventually, the flow exits the heat sink at the foam tip.

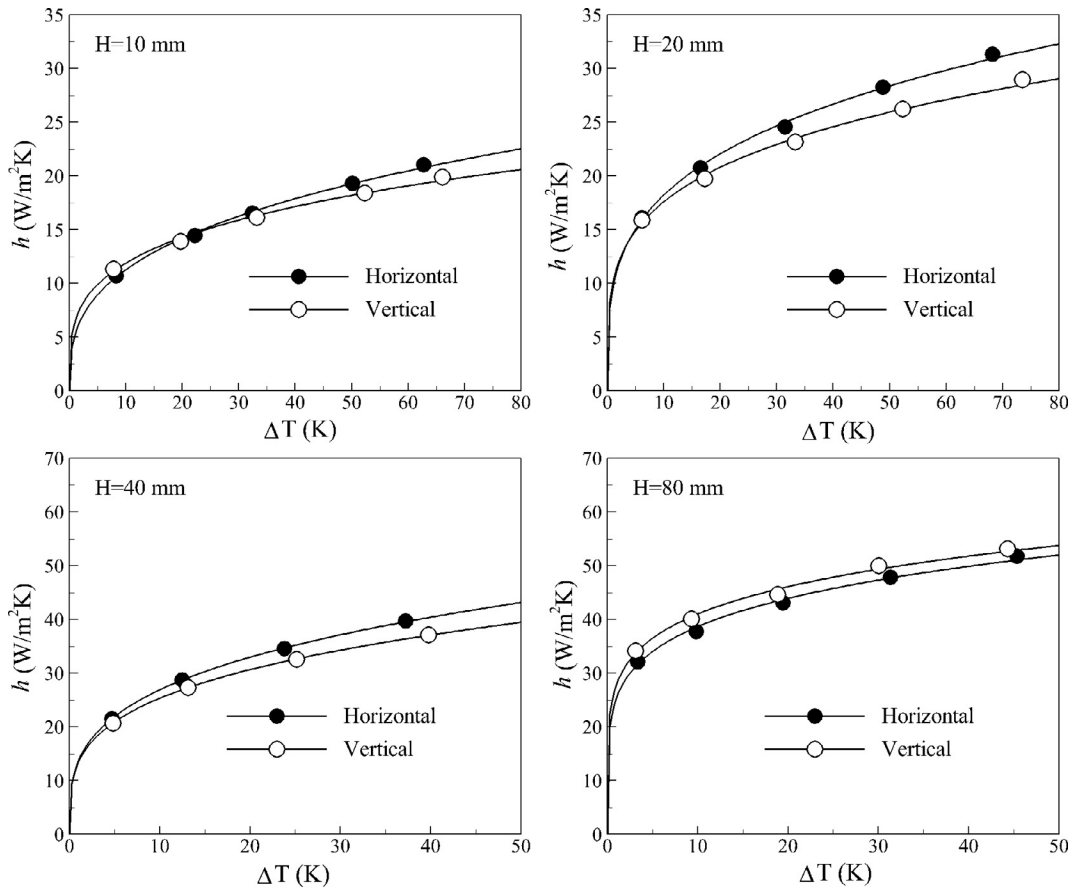


Fig. 11. Comparison of heat transfer coefficients between vertical and horizontal orientations for selected foam heights of 10/20/40/80 mm, with foam strip number $N = 6$.

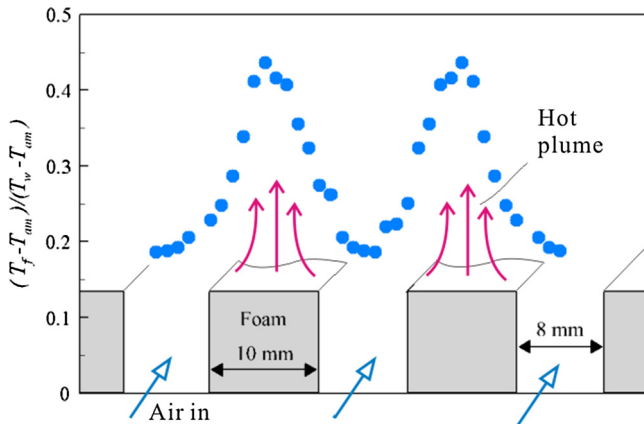


Fig. 12. Air temperature distribution above heat sink revealing flow dynamics in metal foam heat sinks with open slots.

It should be noted that the air temperature measurement was used to assess the overall flow field of natural convection. It was not designed to obtain the quantitative flow field or reveal the subtle distinctions of flow field in foam heat sinks with different parameters. The air temperature distribution of a typical heat sink in Fig. 12 indicates that the fresh air penetrates into the foam strips through the open slots, demonstrating the important role of the open slots in terms of promoting the intake of fresh air into heat sinks in comparison to the conventional foam heat sink with a single foam block. For the vertical orientation, it is believed that the open slots should play a similar role in promoting the intake of fresh air into heat sinks.

4. Conclusion

Natural convection in metal foam heat sinks with open slots was experimentally investigated. The effects of slot width, foam height and heat sink orientation on the thermal performance of the heat sink were systematically studied and the underlying mechanisms explored. Main results were summarized as follows:

- As the width of open slots is increased from zero (corresponding to heat sink with a single foam block), the heat transfer coefficient first increases due to increase in the overall permeability of the heat sink. The heat transfer coefficient then starts to decrease as the slot width is further increased as a result of decreased overall heat transfer area. The optimum slot width was found to be 5–8 mm within the present experimental conditions, regardless of heat sink orientations (horizontal versus vertical).
- The effect of slot width on the heat transfer coefficient decreases with decreasing foam height.
- The heat transfer coefficient is enhanced by increasing foam height due to the larger heat transfer area. However, the rate of enhancement decreases with increasing foam height due mainly to the limited conduction capability of high porosity metal foam.
- Overall, the horizontal orientation yields a higher heat transfer coefficient than that of the vertical orientation for the same heat sink within the investigated range of parameters.
- Air temperature distribution above the heat sink of horizontal orientation reveals that the fresh air penetrates into the foam strips through the open slots, demonstrating the important role

of the open slots in terms of promoting the intake of fresh air into heat sinks in comparison to the conventional foam heat sink with a single foam block.

Acknowledgements

This work was supported by the National Natural Science Foundation of China (51676156, 51206128), the National “111” Project of China (B06024), the Postdoctoral Science Foundation of China (2016M590942), the Shaanxi Province Science Foundation, and the Fundamental Research Funds for the Central Universities of China.

References

- [1] J. Petroski, Advanced natural convection cooling designs for light-emitting diode bulb systems, *J. Electron. Packag.* 136 (4) (2014) 041005.
- [2] T. Cheng, X. Luo, S. Huang, Thermal analysis and optimization of multiple LED packaging based on a general analytical solution, *Int. J. Therm. Sci.* 49 (1) (2010) 196–201.
- [3] Q. Shen, D. Sun, Y. Xu, T. Jin, X. Zhao, Orientation effects on natural convection heat dissipation of rectangular fin heat sinks mounted on LEDs, *Int. J. Heat Mass Transf.* 75 (2014) 462–469.
- [4] M. Mehrtash, I. Tari, A correlation for natural convection heat transfer from inclined plate-finned heat sinks, *Appl. Therm. Eng.* 51 (1) (2013) 1067–1075.
- [5] B. Li, Y.J. Baik, C. Byon, Enhanced natural convection heat transfer of a chimney-based radial heat sink, *Energy Convers. Manage.* 108 (2016) 422–428.
- [6] V.A. Costa, A.M. Lopes, Improved radial heat sink for led lamp cooling, *Appl. Therm. Eng.* 70 (1) (2014) 131–138.
- [7] M.A. Almgobel, Constructural tree-shaped fins, *Int. J. Therm. Sci.* 44 (4) (2005) 342–348.
- [8] E. Yu, Y. Joshi, Heat transfer enhancement from enclosed discrete components using pin–fin heat sinks, *Int. J. Heat Mass Transf.* 45 (25) (2002) 4957–4966.
- [9] E. Elshafei, Natural convection heat transfer from a heat sink with hollow/perforated circular pin fins, *Energy* 35 (7) (2010) 2870–2877.
- [10] A. Bejan, D. Poulikakos, The non-darcy regime for vertical boundary layer natural convection in a porous medium, *Int. J. Heat Mass Transf.* 27 (5) (1984) 717–722.
- [11] S.W. Hsiao, P. Cheng, C.K. Chen, Non-uniform porosity and thermal dispersion effects on natural convection about a heated horizontal cylinder in an enclosed porous medium, *Int. J. Heat Mass Transf.* 35 (12) (1992) 3407–3418.
- [12] TAL, Technical architectural lighting with porifera system using metal foam, 2013, <<http://www.tal.be/en/porifera.aspx>>.
- [13] A. Bhattacharya, R. Mahajan, Metal foam and finned metal foam heat sinks for electronics cooling in buoyancy-induced convection, *J. Electron. Packag.* 128 (3) (2006) 259–266.
- [14] G. Hetsroni, M. Gurevich, R. Rozenblit, Natural convection in metal foam strips with internal heat generation, *Exp. Thermal Fluid Sci.* 32 (8) (2008) 1740–1747.
- [15] S.D. Schampheleire, P.D. Jaeger, R. Reynnders, et al., Experimental study of buoyancy-driven flow in open-cell aluminium foam heat sinks, *Appl. Therm. Eng.* 59 (1) (2013) 30–40.
- [16] Z.G. Qu, T.S. Wang, W.Q. Tao, T.J. Lu, Experimental study of air natural convection on metallic foam-sintered plate, *Int. J. Heat Fluid Flow* 38 (2012) 126–132.
- [17] C.Y. Zhao, T.J. Lu, H.P. Hodson, Natural convection in metal foams with open cells, *Int. J. Heat Mass Transf.* 48 (12) (2005) 2452–2463.
- [18] M. Phanikumar, R. Mahajan, Non-Darcy natural convection in high porosity metal foams, *Int. J. Heat Mass Transf.* 45 (18) (2002) 3781–3793.
- [19] S.S. Feng, J.J. Kuang, T. Wen, T.J. Lu, K. Ichimiya, An experimental and numerical study of finned metal foam heat sinks under impinging air jet cooling, *Int. J. Heat Mass Transf.* 77 (2014) 1063–1074.
- [20] S.S. Feng, Y. Zhang, M. Shi, T. Wen, T.J. Lu, Unidirectional freezing of phase change materials saturated in open-cell metal foams, *Appl. Therm. Eng.* 88 (2015) 315–321.
- [21] Frank P. Incropera, De Witt, P. David, *Fundamentals of Heat and Mass Transfer*, John Wiley and Sons Inc, NY, 1985.
- [22] H.W. Coleman, W.G. Steele, *Experimentation and Uncertainty Analysis for Engineers*, second ed., Wiley, NY, 1999.
- [23] X.H. Yang, J.J. Kuang, T.J. Lu, et al., A simplistic analytical unit cell based model for the effective thermal conductivity of high porosity open-cell metal foams, *J. Phys. D Appl. Phys.* 46 (25) (2013) 255302.